Supporting Information

Ferromagnetic resonance biosensor for homogeneous and volumetric detection of DNA

Bo Tian, Xiaoqi Liao, Peter Svedlindh, Mattias Strömberg,* Erik Wetterskog*

Department of Engineering Sciences, Uppsala University, The Ångström Laboratory, Box 534, SE-751 21 Uppsala, Sweden

Table of Contents

Table S1. Sequences of templates and probes used for RCA-based biosensing. *Italicized and underlined* DNA regions are complementary to each other. **Bold and underlined** DNA regions are complementary to each other. ***Bold and italicized*** DNA regions in the padlock and detection probe are identical and therefore indicate the binding position of the detection probe in the RCA product.

Name	Sequence (**5'→3'**)
Vibrio cholerae target	*CCCTGGGCTCAACCTA***GGAATCGCATTTG**
Padlock probe	Phosphate-*TAGGTTGAGCCCAGGG*ACTTCTAGAGTGTACCGACCTCAGTAG CCGTGACTATCGACT*TGTTGATGTCATGTGTCGCAC***CAAATGCGATTCC**
Detection probe	Biotin-TTTTTTTTTTTTTTTTTTTT*TGTTGATGTCATGTGTCGCAC*

Table S2. Sequences of target DNA (a 230 bp highly conserved region of ZIKV NS5 protein gene, GenBank accession number: KM078929-KM078979), outer primers (F3/B3), inner primers (FIP/BIP) and loop primers (LF/LB) used for LAMP-based biosensing.

Name	Sequence (**5'→3'**)
Target DNA	CAACGGATGGGATAGGCTCAAACGAATGGCAGTCAGTGGAGATGATTGCGTTGTGAAGCCAATTGATGATAGGTTTGCACATGCCCTCAGGTTCTTGAATGATATGGGAAAAGTTAGGAAGGACACACAAGAGTGGAAACCCTCAACTGGATGGGACAACTGGGAAGAAGTTCCGTTTTGCTCCCACCACTTCAACAAGCTCCATCTCAAGGACGGGAGGTCCATTGTGG
F3	CGGATGGGATAGGCTCAAAC
B3	ATGGACCTCCCGTCCTTG
FIP	CCTGAGGGCATGTGCAAACCTAGAATGGCAGTCAGTGGAGAT
BIP	ACCCTCAACTGGATGGGACAACTGGAGCTTGTTGAAGTGGTG
LF	CATCAATTGGCTTCACAACGC
LB	GGGAAGAAGTTCCGTTTTGCTC
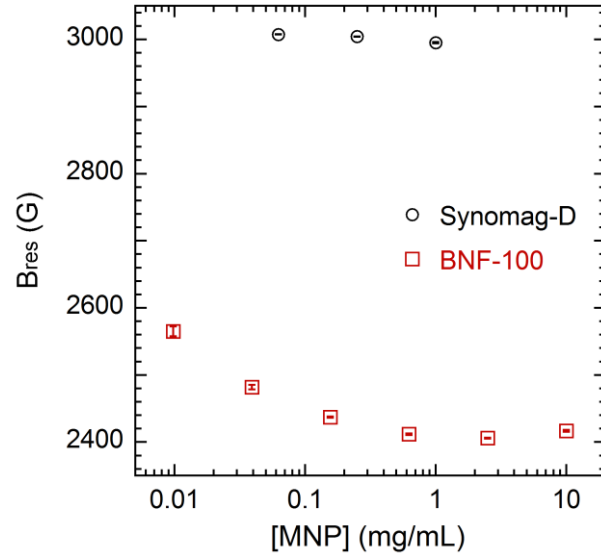
Figure S1. Variation of B_{res} with MNP concentration. For BNF-100 MNPs (red squares), the decrease of B_{res} with increasing MNP concentration is a clear signature of magnetic field-induced chaining of individual MNPs. At higher BNF-100 MNP concentrations, formation of a higher number or longer MNP chains occurs leading to an increase of the effective (shape) anisotropy of the system, and a concomitant decrease of B_{res}. For the 56 nm magnetic nanoflowers (synomag-D, black circles), only a slight decrease of B_{res} with increasing particle concentration is observed. Error bars indicate the standard deviation of three independent replicates.
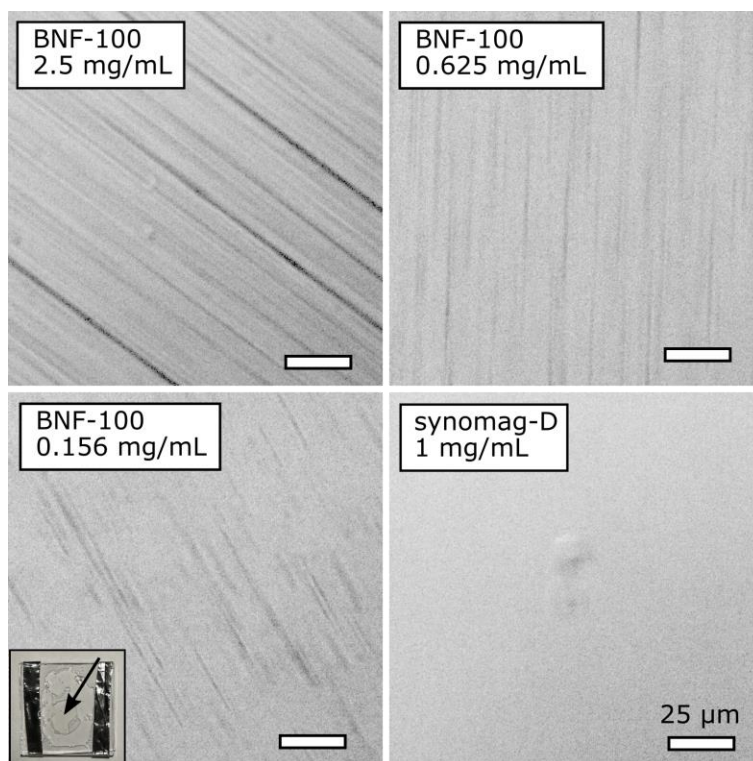
Figure S2. Observation of BNF-100 chains in an optical microscope. Representative top-view images of MNP chains formed in a magnetic field of 1000 G, provided by a circular Halbach array. For the 56 nm magnetic nanoflowers (synomag-D), no chains are observed in a magnetic field of 1000 G. The faint contrast in the image comes from debris at the interface. The inset shows an example of a sample prepared for observation in the optical microscope. A 3.5 µL drop is sandwiched between two glass slides. Two strips of Al-foil were used as spacers, and the droplet was confined within a wall of silicon grease. The arrow indicates position of the thin liquid layer of the MNP dispersion from where the top-view images are taken.
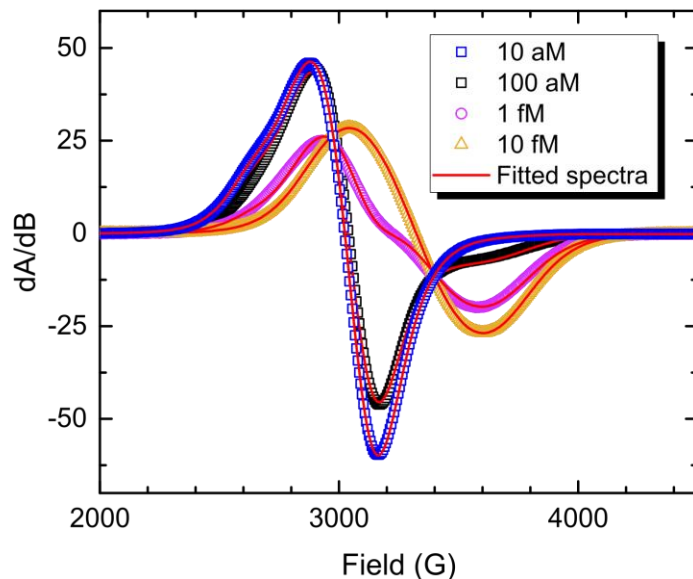
Figure S3. LAMP-FMR spectra (as shown in Figure 5a) fitted using a linear combination approach. Fitting each spectrum as a linear combination of a positive (100 fM target concentration) and negative spectrum (blank control) provides a more quantitative measure on the degree of rotational immobilization of the synomag-D nanoflowers in the suspension. In this particular example, the intermediate 100 aM and 1 fM spectra correspond to 21.3±0.3% and 73.8±2.1% of the dynamic range (R^2 > 0.995), where errors are the standard deviations of triplicate measurements. Similarly, the 10 aM and 10 fM spectra corresponds to 0±0% and 99.8±0.2% of the dynamic range.